

Evolution of Mercury's obliquity

Marie Yseboodt*, Jean-Luc Margot

Department of Astronomy, Cornell University, Ithaca, NY 14853, USA

Received 24 June 2005; revised 3 November 2005

Available online 17 February 2006

Abstract

Mercury has a near-zero obliquity, i.e. its spin axis is nearly perpendicular to its orbital plane. The value of the obliquity must be known precisely in order to constrain the size of the planet's core within the framework suggested by Peale [Peale, S.J., 1976. *Nature* 262, 765–766]. Rambaux and Bois [Rambaux, N., Bois, E., 2004. *Astron. Astrophys.* 413, 381–393] have suggested that Mercury's obliquity varies on thousand-year timescales due to planetary perturbations, potentially ruining the feasibility of Peale's experiment. We use a Hamiltonian approach (free of energy dissipation) to study the spin–orbit evolution of Mercury subject to secular planetary perturbations. We can reproduce an obliquity evolution similar to that of Rambaux and Bois [Rambaux, N., Bois, E., 2004. *Astron. Astrophys.* 413, 381–393] if we integrate the system with a set of initial conditions that differs from the Cassini state. However the thousand-year oscillations in the obliquity disappear if we use initial conditions corresponding to the equilibrium position of the Cassini state. This result indicates that planetary perturbations do not force short-period, large amplitude oscillations in the obliquity of Mercury. In the absence of excitation processes on short timescales, Mercury's obliquity will remain quasi-constant, suggesting that one of the important conditions for the success of Peale's experiment is realized. We show that interpretation of data obtained in support of this experiment will require a precise knowledge of the spin–orbit configuration, and we provide estimates for two of the critical parameters, the instantaneous Laplace plane orientation and the orbital precession rate from numerical fits to ephemeris data. Finally we provide geometrical relationships and a scheme for identifying the correct initial conditions required in numerical integrations involving a Cassini state configuration subject to planetary perturbations.

© 2006 Elsevier Inc. All rights reserved.

Keywords: Interiors; Mercury; Planetary dynamics; Rotational dynamics; Resonances

1. Introduction

Mercury's orbit is not fixed in space but precesses because of torques exerted by planets exterior to its orbit. To first order, if we consider perturbations of the planets on Mercury but neglect mutual interactions between planets, Mercury's orbit precesses with a period of about 235 kyr and a constant inclination with respect to a plane called the Laplace plane. Mercury's spin vector is also expected to precess if the planet is a Cassini state, an evolved rotational state where the spin axis, orbit normal, and normal to the Laplace plane are coplanar while the obliquity remains constant (Colombo, 1966; Peale, 1969, 1988). In order to maintain coplanarity in the Cassini state, the spin axis precesses at the same rate as the orbital plane (see, e.g., Ward, 1975; Gladman et al., 1996). Radar measurements (Pettengill and

Dyce, 1965) revealed Mercury's unusual 3:2 spin–orbit resonance: the orbital period (~ 88 days) is exactly $3/2$ of the spin period (~ 59 days).

Provided that the planet is in a Cassini state, Peale (1976) has shown that the knowledge of the second degree coefficients of the gravity field, the 88-day libration amplitude, and the obliquity can be used to determine the state and size of the Hermean core. While the knowledge of the 88-day libration amplitude and C_{22} gravitational harmonic are sufficient to distinguish a molten core from a solid core (Margot et al., in preparation), the combination of all four quantities above is needed to evaluate the moment of inertia C and the ratio C_m/C between the moment of inertia of the mantle and the moment of inertia of the entire planet. This ratio with assumptions on mantle and core densities can be used to constrain the size of the core. Therefore a good description of the obliquity behavior is essential to infer the radius of Mercury's core, which is itself critical to further our understanding of terrestrial planet formation and evolution.

* Corresponding author.

E-mail address: mariey@astro.cornell.edu (M. Yseboodt).

One of the goals of both the MESSENGER (Solomon et al., 2001) and Bepi-Colombo missions (Milani et al., 2001) is to determine these quantities (gravity field, librations, obliquity) for Mercury. Earth-based radar data can also be used to determine the libration amplitude and the instantaneous spin orientation.

The idealized situation in Peale's experiment can be complicated by the presence of free modes of rotation. A free mode has an arbitrary phase and amplitude but its frequency is fixed. Possible free modes are a libration in longitude which produces a variation of the rotation angle about the spin axis with a period of order 15 years (Peale, 1974) and a precession which moves the spin axis around the Cassini state with a period of order 1000 years (Colombo, 1966; Peale, 1974). A free libration in longitude would not affect the obliquity nor the ability to distinguish a molten from a solid core. But a free precession would change the orientation of the spin axis in space and therefore the obliquity value, potentially ruining the ability to determine the radius of the core in Peale's experiment.

Peale (2005) examined the free rotational motions of Mercury and their damping by considering tidal friction and dissipation at the core–mantle interface. He derived damping timescales for these modes of about 10^5 years, much shorter than the age of the Solar System. If the free modes are detected in the spin state measurements, it will indicate an active or recent excitation mechanism, as the amplitude of the free modes should decay on $\sim 10^5$ year timescales.

Rambaux and Bois (2004) have suggested that planetary perturbations cause obliquity variations on thousand-year timescales, much less than the 10^5 year damping timescales. Their numerical integrations show that Mercury's obliquity is not constant with time. The authors find variations of a few arcminutes around a mean value of about 1.6 arcmin at a proper frequency of 1066 years, corresponding to the free precession period for the values of moments of inertia they chose. For a rigid body, the free precession frequency ν_P is given to first order by the equation

$$\nu_P = n \frac{C - (A + B)/2}{C} \quad (1)$$

which follows from Euler's equations for rigid-body rotation. In this equation, n is the mean motion, A , B and C the moments of inertia. An expression for the precession frequency that takes the triaxial shape and the resonant rotation of Mercury into account is given by Peale (2005). The free libration period similarly depends on the moments of inertia.

In this paper, we investigate the value of the obliquity and its time evolution. We use a Hamiltonian formulation which includes secular planetary perturbations but no internal energy dissipation to compute the spin–orbit motion of Mercury. The formalism is described in Section 2. Readers who are not interested in Hamiltonian mechanics can proceed to Section 3 without too much loss of continuity. Section 3 is devoted to the determination of the Laplace plane which is central to this problem and to the definition of the Cassini state. In Section 4, we present geometrical relationships between the obliquity and other variables defining the Cassini state. Results of the numerical integrations of the system are presented in Section 5,

including one simulation that reproduces the oscillations in the obliquity seen by Rambaux and Bois (2004). We find that integrations started in the Cassini state do not exhibit oscillations. In Section 6, we present a practical way to numerically find the position of the Cassini state and the associated obliquity. The equilibrium obliquity—important for the interpretation of future Mercury geodesy data—depends on the values of the moments of inertia and other parameters, which we investigate in Section 7.

2. Method

One way to study the spin–orbit motion of Mercury is to numerically integrate the motions of the planets of the Solar System with a relativistic integrator (e.g., Rambaux and Bois, 2004). Another way is to use a simplified analytical approach. In a masterful paper, D'Hoedt and Lemaître (2004) obtain the equilibrium solutions and the frequencies of the spin-axis motion by using Hamilton's equations. In order to maintain a tractable Hamiltonian with two degrees of freedom, those authors make the following simplifications: principal axis rotation, a description of the gravity field limited to second degree and order terms, no planetary perturbations, no tides nor damping, and all the perturbations with period equal or smaller to the revolution period (88 days) are neglected.

For the convenience of the reader, we briefly describe the reference frames and the Andoyer and Delaunay variables that are used in the development of the Hamiltonian. Additional details can be found in D'Hoedt and Lemaître (2004). The reference frame X_0, Y_0, Z_0 is based on the ecliptic plane at epoch J2000. This choice of reference frame allows us to easily add planetary perturbations. The frame tied to the orbital plane is denoted by X_1, Y_1, Z_1 , the frame tied to the spin orientation is denoted by X_2, Y_2, Z_2 , and the frame tied to the principal axes of inertia is denoted by X_3, Y_3, Z_3 .

The Andoyer variables (l, g, h, L, G, H) (Deprit, 1967) describe the rotation of Mercury. Three lowercase symbols represent angles and three uppercase symbols represent conjugated momenta: $g + l$ is the angle between X_2 and the axis of minimum inertia X_3 , h is the angle between X_0 and X_2 (the longitude of the ascending node of the spin in the ecliptic frame), G is the norm of the spin angular momentum of Mercury, $H = G \cos K$ is the projection of the angular momentum vector on the inertial axis Z_0 where we define K as the angle between Z_0 and Z_2 (the inclination of the spin axis with respect to the ecliptic plane), and L is the projection of the angular momentum on Z_3 and is equal to G because of the assumption of principal axis rotation. The non-singular Andoyer variables are given by $\Lambda_1 = G$ and $\Lambda_3 = G(1 - \cos K)$, $\lambda_1 = l + g + h$ and $\lambda_3 = -h$.

The Delaunay variables ($l_0, g_0, h_0, L_0, G_0, H_0$) express the revolution of Mercury with respect to the inertial frame. They are related to the planetary orbital elements with the momenta $L_0 = m\sqrt{G(M+m)a_0}$, $G_0 = L_0\sqrt{1 - e_0^2}$, $H_0 = G_0 \cos i_0$, where m is the mass of Mercury, M is the mass of the Sun, and G is the gravitational constant when it appears in front of a mass symbol. The corresponding angles are as follows: l_0

is the mean anomaly, $g_0 = \omega_0$ is the argument of pericenter, and $h_0 = \Omega_0$ is the longitude of the ascending node. The semi-major axis, eccentricity and inclination of the orbit with respect to the J2000 ecliptic plane (X_0, Y_0, Z_0) are denoted with the usual symbols a_0, e_0 and i_0 , respectively.

The obliquity θ can be computed from a combination of Andoyer variables and orbital elements:

$$\cos \theta = \cos i_0 \cos K + \sin i_0 \sin K \cos(\Omega_0 - h). \quad (2)$$

We have reproduced the development of the Hamiltonian derived by D'Hoedt and Lemaître (2004) using a mathematical software for symbolic computation. After some canonical transformations and development in the eccentricity up to order 3, the Hamiltonian contains several thousands terms and can be shortened by averaging in the fast varying angles (the mean anomaly l_0 and λ_1). The remaining terms include only the long period angles (h, h_0 and g_0) and the spin-orbit resonant angle ($\lambda_1 - \frac{3}{2}l_0$). The final Hamiltonian with two degrees of freedom is included here for convenience:

$$\begin{aligned} H_2 = & \frac{\Lambda_1^2}{2C} - \frac{m^3 \mu^2}{2(\Lambda_0 - \frac{3\Lambda_1}{2})^2} \\ & - \frac{GMm^7 \mu^3 R^2}{(\Lambda_0 - \frac{3\Lambda_1}{2})^6} \left[\frac{1}{2} C_{20} \left(1 + \frac{3e_0^2}{2} \right) \right. \\ & \times \left(-\frac{1}{4}(-1 + 3\cos^2 i_0)(-1 + 3\cos^2 K) \right. \\ & - \frac{3}{4}(1 - \cos^2 i_0)(1 - \cos^2 K) \cos(2\sigma_3) \\ & \left. \left. - 3\cos i_0 \cos K \cos \sigma_3 \sin i_0 \sin K \right) \right. \\ & + 3C_{22} \left(\frac{7e_0}{2} - \frac{123e_0^3}{16} \right) \\ & \times \left(\frac{1}{16}(1 + \cos i_0)^2(1 + \cos K)^2 \cos(2\sigma_1) \right. \\ & + \frac{1}{16}(1 - \cos i_0)^2(1 - \cos K)^2 \cos(2\sigma_1 + 4\sigma_3) \\ & + \frac{1}{4}(1 + \cos i_0)(1 + \cos K) \cos(2\sigma_1 + \sigma_3) \sin i_0 \sin K \\ & + \frac{1}{4}(1 - \cos i_0)(1 - \cos K) \cos(2\sigma_1 + 3\sigma_3) \sin i_0 \sin K \\ & \left. \left. + \frac{3}{8} \cos(2\sigma_1 + 2\sigma_3) \sin^2 i_0 \sin^2 K \right) \right], \quad (3) \end{aligned}$$

where $\mu = G(m + M)$, $\sigma_1 = \lambda_1 - \frac{3}{2}l_0 - h_0 - g_0$, $\sigma_3 = h_0 - h$, $\cos K = 1 - \frac{\Lambda_3}{\Lambda_1}$, $\Lambda_0 = L_0 + \frac{3}{2}\Lambda_1$, C_{20} and C_{22} are the second-degree gravitational harmonics, C is the polar moment of inertia and R is the radius of Mercury. The angles σ_1 and σ_3 are the main angles in this problem. They are canonical variables that have been chosen in order to reduce the complexity of the Hamiltonian. Their geometrical significance is not straightforward, since these angles are not defined in a single plane. Roughly speaking, σ_1 is the angle related to the libration in longitude while σ_3 (the difference between the longitude of the

ascending node of the orbit and that of the spin axis) is the angle related to the spin precession.

At this point the Hamiltonian does not capture the precession of the orbital plane because planetary perturbations are not included. In order to take these effects into account, we add the secular parts of the perturbing potential for 7 exterior planets (Murray and Dermott, 1999). We make use of the same variables, same canonical transformations and same assumptions: 3:2 resonance, no small period terms, no dissipation. The perturbing potential is given by

$$\begin{aligned} R_{\text{sec}} = & \sum_{k=1}^7 \frac{Gm_k \alpha_k}{8a_k} \left(b_{3/2}^{(1)} e_0^2 - 4 \sin^2 \frac{i_0}{2} b_{3/2}^{(1)} \right. \\ & - 2e_0 e_k \cos(\varpi_0 - \varpi_k) b_{3/2}^{(2)} \\ & \left. + 8 \sin \frac{i_0}{2} \sin \frac{i_k}{2} \cos(\Omega_0 - \Omega_k) b_{3/2}^{(1)} \right), \quad (4) \end{aligned}$$

where m_k is the mass of planet k , b are the Laplace coefficients, $a_k, e_k, i_k, \varpi_k, \omega_k$ and Ω_k are the semi-major axis, eccentricity, inclination, longitude of the pericenter, argument of pericenter and longitude of the ascending node of the planet k , respectively (the subscript 0 represents Mercury's elements), and $\alpha_k = a_0/a_k$. We then replace in the full Hamiltonian the orbital elements of Mercury with the appropriate Delaunay variables. By subtracting¹ R_{sec} from H_2 , we obtain a Hamiltonian with 4 degrees of freedom. The two additional degrees of freedom come from the two pairs of orbital elements (ω_0, e_0) and (Ω_0, i_0) which now exhibit secular changes due to the planetary perturbations. The four angle combinations and their conjugated momenta are (σ_1, Λ_1) , (σ_3, Λ_3) , $(h_0, H'_0 = H_0 + \Lambda_1 - \Lambda_3)$, and $(g_0, G'_0 = G_0 + \Lambda_1)$.

The three Euler angles defining the orientation of the body axes in the ecliptic frame can be expressed as a function of the canonical variables:

$$\begin{aligned} (h, K, g + l) = & \left(h_0 - \sigma_3, \arccos \left(1 - \frac{\Lambda_3}{\Lambda_1} \right), \right. \\ & \left. \sigma_1 + \sigma_3 + \frac{3}{2}l_0 + g_0 \right). \quad (5) \end{aligned}$$

We numerically integrate Hamilton's equations with respect to the 8 canonical variables and track the time evolution of both the spin-orbit variables ($\sigma_1, \Lambda_1, \sigma_3, \Lambda_3$) and Mercury's orbital elements ($i_0, e_0, \Omega_0, \omega_0$). Our initial conditions for the planetary elements at epoch J2000 were computed by Standish et al. (1992, Table 5.8.1). We use the C_{20} and C_{22} numerical values from the Anderson et al. (1987) analysis of Mariner 10 radio science data.

The secular potential induces a retrograde precession of the orbital plane. The argument of pericenter ω_0 precesses in the prograde direction twice as fast as the longitude of the ascending node Ω_0 regresses, while the eccentricity e_0 and inclination i_0 vary quasi-periodically. However, over the few thousand-year

¹ The subtraction is required because the perturbing potential is defined with the sign opposite to that normally used in a potential ($\sim -GM/r$) (Brouwer and Clemence, 1961).

timescale relevant to the problem, the four osculating elements of Mercury have a roughly linear behavior.

Although our secular potential is clearly a simplification of reality, it is adequate for the purpose at hand. On a timescale of a few kyr, the secular potential captures most of the influences due to exterior planets. Our goal is not to include all the possible effects but to investigate how the motion of Mercury is affected by external perturbers. When using the Hamiltonian formalism, we neglect mutual perturbations between the planets and assume that the orbital elements of the perturbers remain constant with time. These assumptions are justified for the timescales of interest in this work. Relevant timescales are described in more detail in Section 3.2. The short-period terms disappear from the Hamiltonian because of the averaging process. The influence of these terms can be safely neglected in our computations because they induce changes in the rotation variables that have very small amplitudes (\sim a few arcsec). Additional justifications for our assumptions are given at the end of Section 5. We also neglect smaller corrections such as general relativistic effects.

3. Position of the Laplace plane

There have been confusions in recent literature about the plane that is relevant in the Cassini problem. Neither the ecliptic nor the invariable plane (the plane perpendicular to the angular momentum of the Solar System) properly identify the Cassini state. Here we compute the position of the relevant reference plane called the Laplace plane.

In an idealized system it would be the plane about which the orbital inclination remains constant throughout the precessional cycle. In practice it is the plane about which variations in orbital inclination are minimized. We describe three determinations of the Laplace plane, one based on the secular theory, one based on numerical fits to ephemerides, and one based on an analytical formulation.

3.1. Secular theory

The analytical solution is obtained by computing the secular perturbations from all the planets on Mercury's orbit. It is fully consistent with our Hamiltonian formulation but not as accurate as the numerical solution. If we let $p_k = \sin \Omega_k \sin i_k$ and $q_k = \cos \Omega_k \sin i_k$ and assume small planetary inclinations ($\cos i_k/2 \sim 1$), the secular perturbing potential (4) becomes

$$R_{\text{sec}} = \sum_{k=1}^7 \frac{Gm_k a_0}{8a_k^2} (b_{3/2}^{(1)} e_0^2 - (p_0^2 + q_0^2) b_{3/2}^{(1)}) - 2e_0 e_k \cos(\varpi_0 - \varpi_k) b_{3/2}^{(2)} + 2p_k p_0 b_{3/2}^{(1)} + 2q_k q_0 b_{3/2}^{(1)}. \quad (6)$$

Following Burns et al. (1979), we define a precession frequency due to each exterior planet k as

$$w_k = \frac{m_k a_0^2 n b_{3/2}^{(1)}}{4M a_k^2}, \quad (7)$$

where n is the mean motion of Mercury. The sum of these precession rates w_k yield the precession rate of Mercury's orbit, with a period of about 235 kyr. The Lagrange planetary equations for Mercury's p and q values are

$$\dot{q}_0 = \sum_{k=1}^7 (p_k - p_0) w_k, \quad \dot{p}_0 = \sum_{k=1}^7 (q_k - q_0) w_k. \quad (8)$$

The Laplace plane for Mercury is the plane for which $\dot{p}_0 = \dot{q}_0 = 0$:

$$p_0 = \frac{\sum p_k w_k}{\sum w_k}, \quad q_0 = \frac{\sum q_k w_k}{\sum w_k}. \quad (9)$$

This determination of the position of the Laplace plane is fully consistent with our formulation for including planetary perturbations in the Hamiltonian without mutual interactions. The coordinates of the normal to the Laplace plane in J2000 ecliptic coordinates are

$$\lambda_{\text{sec}} = -8.8^\circ, \quad \beta_{\text{sec}} = 87.9^\circ, \quad (10)$$

where λ is the ecliptic longitude and β the ecliptic latitude. With the simple secular potential, the inclination i between Mercury's orbit and the Laplace plane remains quasi-constant. Our solution for the position of the Laplace plane differs from the invariable plane by about 1° (Fig. 1) while the angular distance between the Laplace pole and the ecliptic pole is about 2.1° . Errors in the position of the Laplace plane translate into errors on the position of the Cassini state that are about 2 orders of magnitude smaller due to the 1 in 200 proportion between the obliquity (~ 1.5 arcmin) and the angle between the Laplace pole and the orbit pole ($i \simeq 5.33^\circ$). However, if the ecliptic plane or the invariable plane is erroneously used in the Cassini problem, the error on the Cassini state position can be of order 0.1 arcmin.

We have verified numerically that the orbit pole from our integrations precesses around the Laplace pole in a regular manner in about 235 kyr. The inclination remains within 0.2 arcmin of 5.33° . Since the secular Laplace plane is inclined by about 2.1° with respect to the ecliptic pole, the instantaneous precession frequency around the ecliptic pole is not constant and its instantaneous value varies between 150 and 320 kyr. Averaged over one cycle, the precession period around the ecliptic pole is ~ 235 kyr, as expected.

3.2. Numerical fits to ephemerides

A simplified description of the orbital motion that neglects the coupling between planets is a logical first step in studying the dynamics of the Cassini state for Mercury. This approach was adopted by Peale (1969, 1974) who considered a single precession frequency. In reality the motion of Mercury is more complex. For example, mutual perturbations between planets yield variations in the orbital elements and it is no longer possible to define a plane about which the inclination remains constant. If the coupling between the planets is taken into account, two eigen modes with periods of ~ 230 and ~ 184 kyr dominate influences on the orbital motion of Mercury (e.g., Brouwer

and van Woerkom, 1950), producing a beat frequency of about $(900 \text{ kyr})^{-1}$. The fastest variations in orbital elements occur on $\sim 70 \text{ kyr}$ timescales, as indicated by the highest frequency modes in the Laskar (1988) series.

The complex motion of the orbital plane can be approximated at any given time by precession about a specific axis. We use this property to define an *instantaneous Laplace plane* that is inclined with respect to the orbit by an angle ι . The plane is chosen such that over a few kyr, variations in orbital inclination with respect to the Laplace plane are minimized in a least-squares sense. We argue that this plane defines the current location of the Cassini state. The system is driven by tidal torques and naturally evolves towards a Cassini state defined by this instantaneous Laplace plane.

We numerically estimate the position of the instantaneous Laplace plane near the J2000 epoch. We extract the orbital orientation from the 20 kyr DE408 ephemerides computed by Myles Standish and evaluate the instantaneous Laplace plane positions over time intervals of ± 1 , ± 2 , ± 4 , and $\pm 8 \text{ kyr}$ around J2000. As expected, the approximation of simple precession about a fixed axis degrades with increasing duration of the time interval. The best fit value for the Laplace pole over a $\pm 1 \text{ kyr}$ interval in the ecliptic frame of J2000 is

$$\lambda_{\text{inst}} = 66.6^\circ, \quad \beta_{\text{inst}} = 86.725^\circ \quad (11)$$

for which the rms inclination deviation is 0.14 arcsec over 2 kyr.

The position of the Laplace pole is constrained fairly well in one dimension (the direction of the orbit pole trajectory projected on the ecliptic plane) but not in the orthogonal dimension (Fig. 1). This is due to the fact that we fit a precessional motion with period $\sim 300 \text{ kyr}$ with a data set that spans 2 kyr. We compute error bars on the Laplace pole position as follows. For each trial pole (λ, β) , we find the inclination ι that minimizes inclination deviations in an rms sense. A 68.3% confidence region is given by the locus of poles for which the sum of squares of residuals is less than 3.3 times that of the best-fit solution. This criterion was used to compute the confidence region in Fig. 1. One-sigma uncertainties along the major and minor axes of the ellipse are 1.5° and 1 arcmin. Despite seemingly large uncertainties, the prospects for the interpretation of future geodesy measurements remain good. The uncertainty on the Laplace pole does not affect the coplanarity condition of the Cassini state appreciably (Section 4) because the J2000 orbit pole orientation is aligned with the long axis of the Laplace pole uncertainty region (Fig. 1).

We perform similar Laplace plane determinations with 1500 years of SONYR data provided by Nicolas Rambaux and with the Laskar (1988) orbital element series. Our best fit value for the instantaneous Laplace plane using the DE408 values, Laskar series and SONYR integrations are all within 0.4° of each other and are valid for a few hundred years around J2000. We note that the instantaneous Laplace plane (11) is 3.4° from the secular solution (10). The former is required for precise interpretation of future ground-based and spacecraft data, while the latter is required for consistency when using a simplified secular potential to describe the spin-orbit motion.

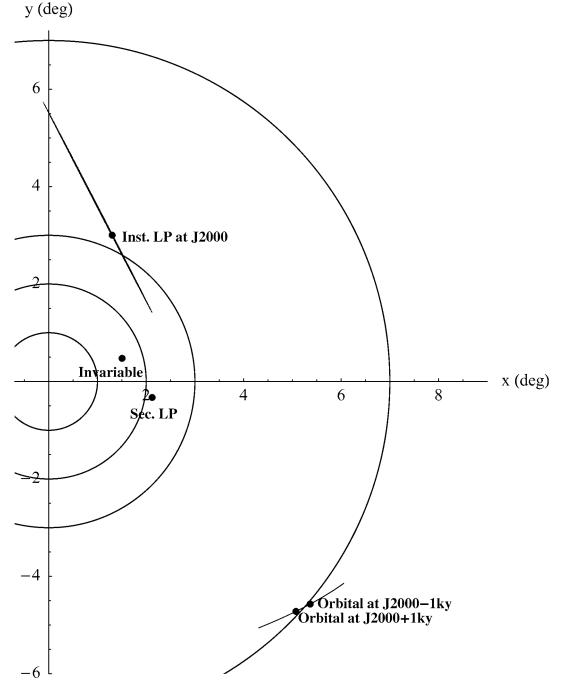


Fig. 1. Positions of poles relevant to the Cassini problem projected on the J2000 ecliptic plane. Our determinations of the secular Laplace pole LP (10) and the instantaneous Laplace pole based on DE408 data (11) are shown. The position of the orbital pole (Standish, DE408) and of the invariable pole (Owen, 1990) are also shown. The narrow cloud of points near the instantaneous Laplace pole at J2000 represents a 68.3% confidence region for that pole.

In addition to the position of the Laplace pole, two related quantities can be evaluated and are needed to compute the equilibrium obliquity in the Cassini state. The orbital precession rate μ around the Laplace pole corresponds to an instantaneous period of about 328 kyr and the angle ι is about 8.6° . These two quantities are highly correlated: when the inclination ι increases, the precession rate decreases. Both quantities are affected by the uncertainty on the Laplace pole, yielding error bars of 50 kyr and 1.2° on the period and angle, respectively. Peale (1981) has proposed an analytical expression to compute the value of the equilibrium obliquity in the Cassini state θ_{CS} :

$$\theta_{\text{CS}} = - \frac{C\mu \sin \iota}{C\mu \cos \iota + 2nmR^2 \left(\frac{7}{2}e_0 - \frac{123}{16}e_0^3 \right) C_{22} - nmR^2 (1 - e_0^2)^{-\frac{3}{2}} C_{20}} \quad (12)$$

This expression is valid only if θ_{CS} is small and is a function of the precession frequency μ , the inclination ι and the moments of inertia through the gravity coefficients C_{20} and C_{22} , which we hold at the nominal Mariner 10 values. Even with the large error bars on μ and ι , the equilibrium obliquity is determined with a small uncertainty. To understand why this is so, note that to first order, the equilibrium obliquity θ_{CS} [Eq. (12)] is proportional to the product $\mu \sin \iota$. Over a given time interval, the orbital pole determines an arc in the ecliptic frame that has a fixed length. The quantity $\sin \iota$ is roughly proportional to the radius of the circle that best fits the orbital pole arc. The precession rate is obtained by the ratio between the angle subtended by the orbital arc as seen from the Laplace pole in the ecliptic plane and the time interval. Therefore the product $\mu \sin \iota$ is

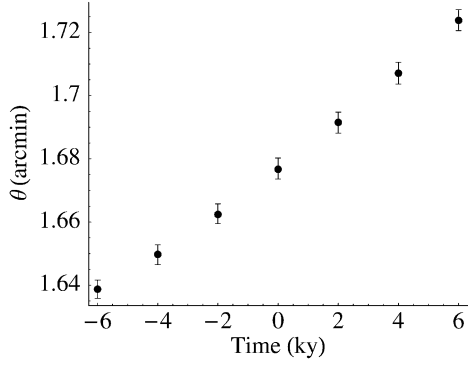


Fig. 2. Time evolution of the equilibrium obliquity estimated over successive 2 kyr intervals from the DE408 ephemerides. The time $t = 0$ corresponds to the J2000 epoch.

constant for all the poles in the direction orthogonal to the orbit pole trajectory. Since the uncertainty region is mainly aligned with the direction orthogonal to the orbit pole trajectory, candidate Laplace poles inside the uncertainty region yield very similar obliquity values, all within 1 arcsec of each other. We can assign uncertainties on the obliquity values by propagating the formal errors on μ and ι through Eq. (12). This assumes that the orbital ephemerides are perfectly known. We find uncertainties less than 1% or 1 arcsec. Peale et al. (2002) have shown that 10% uncertainties on the obliquity measurement are sufficient to yield a 22% precision on the ratio C_m/C between the moments of inertia of the mantle and of the planet.

We can use the 20 kyr timespan of the DE408 ephemeris to study the time evolution of the position of the Laplace pole and other related quantities such as μ , ι and θ_{CS} . We evaluate these quantities using 2 kyr intervals centered on different epochs. The position of the Laplace pole changes by a few degrees in about 20 kyr while the instantaneous precession period increases from ~ 200 to ~ 500 kyr during the same interval. The angle ι also increases with time, from 5° to 13° . The errors bars obtained for each parameter at different epochs are similar to those at the J2000 epoch. Even if the precession rate μ and the inclination ι evolve rapidly over 20 kyr, the equilibrium obliquity variations are small, with a value ranging between 1.64 and 1.72 arcmin (Fig. 2).

3.3. Analytical determination of the Laplace pole

We can compare our numerical results to an analytical determination of the Laplace pole by using an approach similar to Peale (2006). Let us define the position of the orbital pole in the ecliptic frame $\mathbf{x} = \{\sin i_0 \sin \Omega_0, -\cos \Omega_0 \sin i_0, \cos i_0\}$ and its velocity $\mathbf{v} = \frac{d\mathbf{x}}{dt}$. The orbit precesses around an axis defined by the angular velocity of the orbit plane $\mathbf{w} = \{a, b, c\}$ so that $\mathbf{w} \times \mathbf{x} = \mathbf{v}$. By developing \mathbf{w} as a function of i_0 , Ω_0 and their time derivatives, we obtain a general expression for \mathbf{w}

$$\mathbf{w} = \left\{ \frac{di_0}{dt} \cos \Omega_0 + \left(c - \frac{d\Omega_0}{dt} \right) \sin \Omega_0 \tan i_0, \right. \\ \left. \frac{di_0}{dt} \sin \Omega_0 - \left(c - \frac{d\Omega_0}{dt} \right) \cos \Omega_0 \tan i_0, c \right\}. \quad (13)$$

The norm of \mathbf{w} gives the instantaneous precession rate μ around the \mathbf{w} vector while the angle ι is defined by the angle between \mathbf{w} and \mathbf{x} . Equation (13) has one degree of freedom with the free parameter c and defines a curve in space, yielding a family of Laplace poles. One particular value of the parameter $c = -1.91 \times 10^{-5}$ rad/yr appropriate for J2000 yields the coordinates (11) of our Laplace pole determination which minimizes the inclination variations. Our instantaneous Laplace pole is part of a family of solutions for the \mathbf{w} -based definition of the Laplace pole. The equilibrium obliquity is independent of the c parameter (the product $\mu \sin \iota$ is only a function of i_0 , $\frac{di_0}{dt}$ and $\frac{d\Omega_0}{dt}$). Moreover, vectors fulfilling Eq. (13) all belong to the same plane as the orbital vector \mathbf{x} . These two conditions ensure a unique Cassini state position for all \mathbf{w} vectors.

4. Cassini state and initial conditions

We will show that initial conditions play a crucial role when integrating the spin–orbit motion of Mercury. Here we derive geometrical relationships between the quantities defining the Cassini state and we formulate expressions for initial conditions used in our integrations. If the Cassini equilibrium obliquity θ_{CS} is known, we can deduce the position of the spin axis corresponding to the Cassini state which we represent by the vector \mathbf{C} .

The coplanarity condition between the Laplace normal \mathbf{L} , the orbit normal \mathbf{O} and the spin axis in the Cassini state imposes that \mathbf{C} is a linear combination of \mathbf{O} and \mathbf{L} :

$$\mathbf{C} = \alpha \mathbf{O} + \beta \mathbf{L}. \quad (14)$$

Another condition comes from the fact that we define \mathbf{C} , \mathbf{O} and \mathbf{L} as unit vectors:

$$1 = \mathbf{C} \cdot \mathbf{C} = (\alpha \mathbf{O} + \beta \mathbf{L}) \cdot (\alpha \mathbf{O} + \beta \mathbf{L}) \\ = \alpha^2 + \beta^2 + 2\alpha\beta \mathbf{L} \cdot \mathbf{O}. \quad (15)$$

Defining $\gamma = \mathbf{L} \cdot \mathbf{O}$ and solving for β yield

$$\beta = -\alpha\gamma \pm \sqrt{\alpha^2\gamma^2 - \alpha^2 + 1}. \quad (16)$$

Since the obliquity θ_{CS} is the angle between \mathbf{C} and \mathbf{O} , we have

$$\cos \theta_{CS} = \mathbf{O} \cdot \mathbf{C} = \alpha + \beta \mathbf{O} \cdot \mathbf{L}. \quad (17)$$

For each equilibrium obliquity θ_{CS} (4 Cassini states for Mercury, Peale, 1969), we solve for α and β using Eqs. (16) and (17), and we evaluate \mathbf{C} using Eq. (14). The vector \mathbf{C} can be expressed as a function of the inclination of the spin axis in the Cassini state K_{CS} and the longitude of the ascending node h_{CS} , both of which are needed to specify initial conditions for numerical integrations (Table 1). We have

$$\mathbf{C} = \{\sin h_{CS} \sin K_{CS}, -\cos h_{CS} \sin K_{CS}, \cos K_{CS}\}, \quad (18)$$

with angles defined with respect to the J2000 ecliptic frame.

Table 1

Initial conditions for the spin–orbit variables corresponding to the Cassini state (CS) without planetary perturbations (line 1), to the Cassini state with planetary perturbations (lines 2 and 3), and to those of [Rambaux and Bois \(2004\)](#) transformed to our variable set using Eq. (5) (line 4). The relevant epochs are J2000 (line 3) and 1969-07-01 (line 4). In the Cassini state, the rotation frequency is exactly three halves of the revolution frequency n , which dictates the value for the spin angular momentum Λ_1 . σ_1 is the angle related to the libration in longitude. The spin orbit variable σ_3 (the difference in node longitudes) in the Cassini state is equal to $\sigma_{3CS} = h_0 - h_{CS}$, and the associated momentum $\Lambda_{3CS} = \Lambda_1(1 - \cos K_{CS})$. Without planetary perturbations, the obliquity of Cassini state 1 is equal to 0 so that the spin axis is aligned with the orbit normal

	θ arcmin	θ_{CS} arcmin	K deg	σ_1 arcmin	σ_3 arcmin	Λ_1 mR^2/yr	Λ_3 mR^2/yr
CS without planetary perturbations	0	0	i_0	0	0	$\frac{3}{2}Cn$	$\Lambda_1(1 - \cos i_0)$
CS with planetary perturbations	θ_{CS}	θ_{CS}	K_{CS}	0	σ_{3CS}	$\frac{3}{2}Cn$	Λ_{3CS}
	1.5	1.5	7.029	0	2.67	13.306	0.1000
Non-CS equivalent to Rambaux and Bois (2004)	0	1.6	7.005	-3	0	13.305	0.0993

In the integrations that follow, we wish to monitor possible departures from the Cassini state. We define an angle ε that represents the angular deviation between the spin axis \mathbf{S} and the plane formed by the orbit pole \mathbf{O} and Laplace pole \mathbf{L} :

$$\sin \varepsilon = \frac{\mathbf{O} \times \mathbf{L}}{\|\mathbf{O} \times \mathbf{L}\|} \cdot \mathbf{S}. \quad (19)$$

The angle ε is a measure of the proximity of the spin axis orientation to the coplanarity condition of the Cassini state. The spin pole leads the orbit pole when ε is positive while $\varepsilon = 0$ corresponds to the coplanarity condition of the Cassini state. The angle ε should not be confused with the discrepancy between the obliquity and the equilibrium obliquity $\theta - \theta_{CS}$. This last quantity is difficult to evaluate since θ_{CS} is a priori unknown. The Cassini state is reached when both conditions $\theta = \theta_{CS}$ and $\varepsilon = 0$ are fulfilled. The obliquity θ is the angle between \mathbf{S} and \mathbf{O} , hence the spin axis cannot be displaced from the \mathbf{LO} plane by more than θ degrees ($|\varepsilon| \leq \theta$).

Without planetary perturbations, the Cassini state is defined by $\theta = 0$, implying $\varepsilon = 0$. When the planetary perturbations are taken into account, the vectors \mathbf{O} and \mathbf{S} vary with time. Therefore we numerically check at each timestep how close the spin, orbit and Laplace poles are to coplanarity by computing the angle ε .

5. Time evolution of the rotation variables

Having defined the formalism, the location of the Laplace plane, and the initial conditions relevant to the Cassini state, we now tackle the time evolution of the spin–orbit variables.

In the simplest case involving no planetary perturbations, Hamilton's equations with respect to the conjugated variables yield four equilibrium values that correspond to the Cassini states as shown by [Peale \(1974\)](#) and [D'Hoedt and Lemaître \(2004\)](#). One of the solutions, traditionally referred to as Cassini state 1, has zero obliquity. [D'Hoedt and Lemaître \(2004\)](#) have also shown that motion around the equilibrium can be described to first order by a harmonic oscillator. They derive two proper frequencies which are in agreement with the numerical results of [Rambaux and Bois \(2004\)](#). Our development also reproduces the values of the two proper frequencies (1066 and 16 years) for similar assumptions on the moment of inertia [$C = 0.34mR^2$, while A and B are derived from the nominal C_{20} and C_{22} from [Mariner 10 \(Anderson et al., 1987\)](#)].

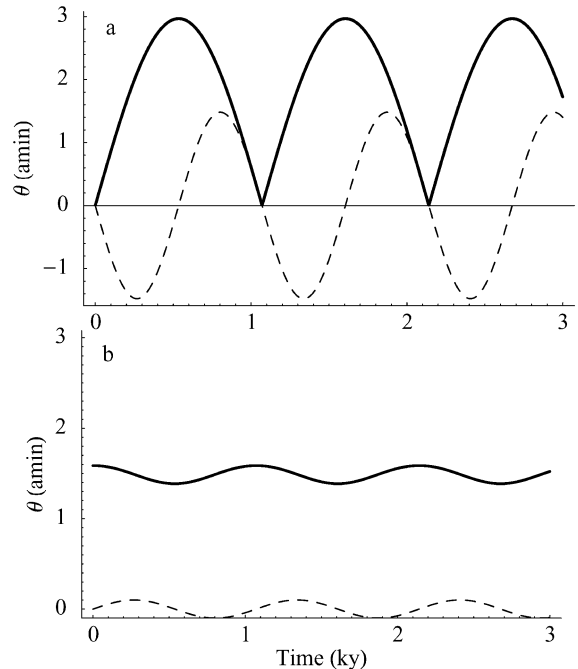


Fig. 3. Variation of Mercury's obliquity over a period of 3000 years with perturbations from external planets. (Top) Evolution with initial conditions identical to those of [Rambaux and Bois \(2004\)](#), where the initial obliquity is 1.6 arcmin away from the equilibrium obliquity. (Bottom) Evolution with an initial obliquity that is 0.1 arcmin away from the equilibrium obliquity. The dashed line is the angle ε that represents deviations from the coplanarity condition of the Cassini state.

Our next step is to reproduce the results of [Rambaux and Bois \(2004\)](#) who use a relativistic integrator for the spin–orbit motion of the 8 planets of the Solar System. In order to do so, we use the averaged Hamiltonian augmented by terms accounting for planetary perturbations. With initial conditions corresponding to those of [Rambaux and Bois \(2004\)](#), we find that the obliquity exhibits oscillations at the ~ 1000 -year period of the free spin precession. Our model reproduces their Fig. 8 ([Fig. 3](#), top). This set of initial conditions ([Table 1](#), line 4) does not correspond to a Cassini state. The time evolution of other rotation variables such as the Euler angles also matches the results of [Rambaux and Bois \(2004\)](#). Both free precession and free libration are present in the solution of the rotation angles. The free libration in longitude changes the rotation velocity but does not affect the obliquity, which is related only to the orientation

of the spin axis is space. The obliquity oscillations are understood as a manifestation of the free precession. The obliquity oscillations maintain a constant amplitude because there is no mechanism for damping free motions in our formalism.

We investigated whether a poor choice of initial conditions for the integration might be responsible for the obliquity variations and we performed integrations with different sets of initial conditions. Although the amplitude of the oscillations is indeed sensitive to initial conditions, we find that substantial obliquity oscillations occur over a wide range of initial conditions. The bottom panel in Fig. 3 shows a set of initial conditions where the initial obliquity is closer to the equilibrium obliquity.

Initial conditions corresponding to the Cassini state do not result in obliquity oscillations. If the system is started at the Cassini state (e.g., Table 1, line 2), the oscillations at the precession frequency do not appear. The libration in longitude angle σ_1 , the spin angular momentum Λ_1 , and the obliquity θ remain quasi-constant while the other spin–orbit angle σ_3 , its conjugated momentum Λ_3 , and the ecliptic inclination K vary with time due to the orbital motion, but without any oscillations. In this situation, the spin axis remains in the Cassini state, even as the equilibrium location changes due to the orbital plane precession. The spin angular momentum Λ_1 is constant because the 88-day forced libration has been averaged out in our formalism.

The interpretation of these results is that planetary perturbations do not excite free modes of rotation with large amplitudes. Rather, deviations from the Cassini state result in a free precession of the spin axis whose signature is apparent in the form of obliquity variations. The only way to avoid the creation of a free precession and the resulting oscillations in obliquity is to start the integration in the Cassini state. The obliquity oscillation is always centered on the equilibrium obliquity and its amplitude is given by the angular deviation from the Cassini state. This deviation is constant with time and may come from an obliquity that is slightly different from the equilibrium obliquity $\theta_{CS} - \theta$, from a deviation from the Cassini state coplanarity ε , or both.

Has Mercury reached the Cassini state? Peale (2005) has shown that the timescale for the damping of the free modes due to internal energy dissipation is $\sim 10^5$ years. This is short with respect to the age of the Solar System but longer than the $\sim 10^4$ year timescale of the Laplace plane reorientation. Therefore the damping may drive the planet towards an equilibrium position that is in fact a moving target and the Cassini state may never be reached. Nevertheless, because the damping timescales are only slightly longer than the orbital variation timescales, and because instantaneous Cassini state positions never deviate far from each other (two orders of magnitude less than angular deviations between instantaneous Laplace planes), we anticipate that the Cassini state has indeed been reached.

What one can say confidently on the basis of our integrations is that if Mercury ever reached the Cassini state, it is likely to have remained in this state, barring recent excitation processes. We show in Section 6 that the planet remains in the Cassini state when the Laplace plane orientation changes smoothly on 10^4 year timescales, or equivalently when planetary per-

turbations are turned on smoothly on 10^4 year timescales. The state is preserved because of torques on the asymmetric planet.

We now reexamine the assumptions of our method. We note that our Hamiltonian formalism does not capture short-period terms due to the averaging process. We argue that the short-period terms cannot produce large obliquity oscillations. For instance, full numerical integrations by Rambaux and Bois (2004) show obliquity curves (their Fig. 11) with short-period oscillations of less than 1 arcsec. Another assumption of our paper is that the mutual interactions between planets can be neglected for the timescale considered (a few kyr). These mutual interactions do not strongly affect the equilibrium value for the obliquity (as shown in Fig. 2) and the position of the Cassini state on those timescales. Over a few thousand years, the obliquity variations computed using DE408 ephemerides are smooth and small (~ 5 arcsec in 12 kyr). The fact that short-period terms and mutual interactions between planets can be neglected on kyr timescales is also supported by the results of Peale (2006). Peale (2006) has shown by using planetary orbital ephemerides averaged over 2000 years that the position of the Cassini state changes with time as expected, that the spin axis remains within 1 arcsec of the Cassini state position, and that no large amplitude oscillations are produced. Additionally he demonstrated that if short-period terms are taken into account, because of the adiabatic invariant theory, the spin axis remains within one arcsec of the Cassini state, provided that the set of initial conditions is chosen in the Cassini state.

To summarize the results of our integrations of the spin–orbit motion in the presence of planetary perturbations, we find that obliquity variations can appear in the form of a free precession if initial conditions do not coincide with a Cassini state. Obliquity variations do not appear when initial conditions are chosen carefully to represent a Cassini state.

6. Equilibrium obliquity in the Cassini state

The previous section illustrates that using initial conditions coinciding with the Cassini state avoids the introduction of oscillations in the spin–orbit evolution. How does one find the correct set of initial conditions? We showed in Section 4 that the Cassini state position can be derived from a knowledge of the equilibrium obliquity θ_{CS} and the orientation of the Laplace plane. Here we describe a numerical technique for obtaining θ_{CS} .

We start with a configuration free of planetary perturbations for which the Cassini state is known and for which the obliquity is zero. We then add planetary perturbations smoothly enough that the system preserves its Cassini state configuration even though the orbital plane starts to precess. The trick consists in turning on the planetary perturbations smoothly by gradually increasing the masses of the perturbers while Mercury's mass remains constant. This effectively prevents the introduction of step functions in the integration. Adding the planetary perturbations abruptly would create free modes as before. Our prescription for the evolution of perturber mass with time is a

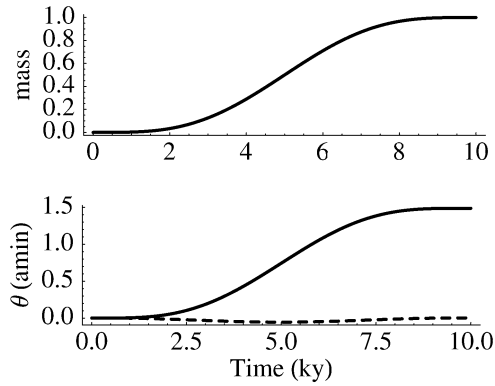


Fig. 4. Our prescription for a smooth evolution of the masses of the perturbers (top) and the corresponding obliquity evolution (bottom) over a period of 10 kyr. The obliquity shows no oscillations when the perturber masses are increased gradually and when the system is started in the perturbation-free Cassini state. The dashed line shows the angle ε (in arcmin) between the spin axis and the plane defined by the normal to the Laplace plane and the normal to the orbital plane, i.e. a measure of the deviation from the coplanarity of the Cassini state. Departures from the Cassini state remain small throughout the integration.

spline function, starting at 0 and ending with the mass of each planet (Fig. 4).

If we choose as initial conditions the Cassini state valid in the absence of planetary perturbations (Table 1, line 1) and gradually increase the perturber masses, we find that oscillations in the obliquity do not arise. Note that the energy of the system is increasing with time in this configuration. The obliquity increases smoothly, with roughly the same functional form as the gradual increase in the masses of the perturbers (Fig. 4). In addition, the spin axis remains very close to the Cassini state throughout the evolution: the spin axis, the normal to the Laplace plane and the normal to the orbital plane remain nearly coplanar. The maximum value for the angle ε is a few arcsec (Fig. 4, dashed line). Due to the relatively fast evolution of the system (~ 10 kyr, only about 10 spin precession periods), the planet is not able to reorient itself fast enough and to keep up with the changes in orbital motion. The planet is driven towards the Cassini state without rotating around it. The quality of the match to the Cassini state improves for longer time constants in the time evolution of the perturber masses. In other words, the gentler the introduction of the perturbations, the closer the system remains to the Cassini state. We find maximal angular deviations from the Cassini state ε of less than 4 arcsec if the time constant for mass increase is about ten times the spin precession period.

We also find that the system follows the Cassini state if we gradually turn off the planetary perturbations by reducing the perturber masses to zero. The obliquity returns to zero without oscillations, starting and ending in the exact, perturbation-free Cassini state.

Finally, we verify that obliquity oscillations appear if the system is integrated from a spin position that is different from a Cassini state, even if planetary perturbations are introduced gently as above. We chose initial conditions with departures from the Cassini state of an arcmin or less and verified that the obliquity exhibits oscillations at the proper frequency of

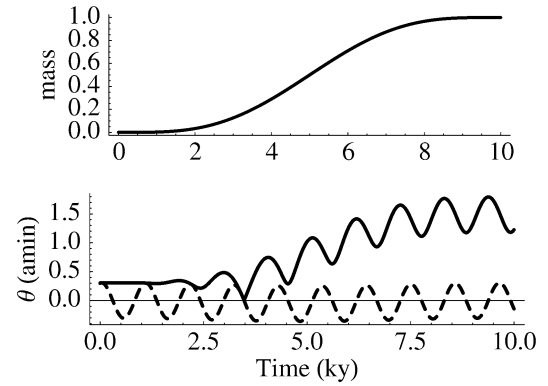


Fig. 5. Evolution of the masses of the perturbers (top) and the corresponding obliquity evolution (bottom) over a period of 10 kyr with initial conditions that do not coincide with a Cassini state. Note obliquity oscillations indicative of free precession. The dashed line represents the angle ε which measures the angular deviation from the strict coplanarity of the Cassini state.

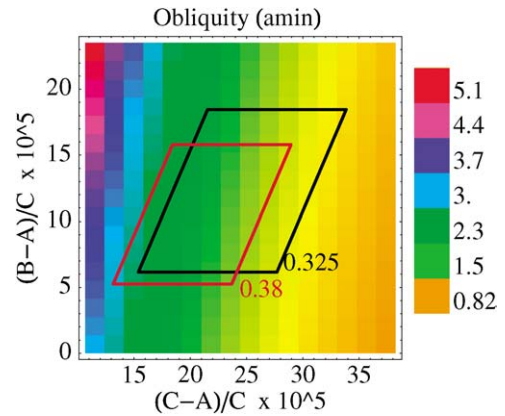


Fig. 6. Obliquity vs the $(B - A)/C$ and $(C - A)/C$ ratios. The black and red boxes show the allowable range for these ratios based on the Mariner 10 gravity data, with $C = 0.325mR^2$ and $C = 0.38mR^2$, respectively.

~ 1000 yr (Fig. 5). Here again, these oscillations are indicative of a free precession.

7. Influence of the moments of inertia on the obliquity

The value of the equilibrium obliquity θ_{CS} is needed to infer the size of the core in Peale's experiment. In this section, we compute how the moments of inertia A , B and C affect the obliquity value and the Cassini state.

We investigate the dependence by numerically integrating Hamilton's equations for different sets of A , B and C with gentle introduction of perturbations to avoid a free precession. As previously noted by Peale (1988), we notice that although the numerical values of the 3 moments of inertia are needed in the Hamiltonian (or equivalently the C , C_{20} and C_{22} values), the obliquity value that we obtain depends only on two combinations of the moments of inertia $(B - A)/C$ and $(C - A)/C$. If we restrict the variations of the moments of inertia to the range of values provided by the Mariner 10 gravity data and the C/mR^2 value to the 0.325–0.38 range encompassing all plausible interior models (Harder and Schubert, 2001), the obliquity can take values between 1.2 and 2.9 arcmin (Fig. 6).

Table 2

This table illustrates that the equilibrium obliquity depends strongly on precession parameters μ and ι . Values computed with Eq. (12) are given for different polar moment of inertia, precession rates and different inclinations between the orbit and the Laplace planes ($\iota = 6.3^\circ$ corresponds to the invariable plane, $\iota = 5.3^\circ$ to the secular Laplace pole and $\iota = 8.6^\circ$ to the instantaneous Laplace pole). The equilibrium obliquity for our best fit values is given in bold and is based on our determination of the instantaneous Laplace plane (Section 3.2). The C_{20} and C_{22} values are those of Anderson et al. (1987)

Precession period (kyr)	Inclination ι ($^\circ$)	θ (arcmin)		
		$C = 0.325mR^2$	$C = 0.34mR^2$	$C = 0.38mR^2$
235	5.3	1.39	1.45	1.63
235	6.3	1.65	1.73	1.93
235	8.6	2.24	2.34	2.62
328	5.3	0.995	1.04	1.16
328	6.3	1.18	1.24	1.38
328	8.6	1.60	1.68	1.87

Our numerical results for the obliquity in the Cassini state can be compared with the solution of the analytical equation (12) where $C_{20} = -\frac{C-(A+B)/2}{mR^2}$ and $C_{22} = \frac{B-A}{4mR^2}$. We note that the solution to Eq. (12)—and therefore the interpretation of future obliquity measurements—is highly dependent on the values chosen for the parameters μ and ι . For A and B values corresponding to the Mariner 10 gravity data and a polar moment of inertia $C = 0.34mR^2$, the obliquity ranges between 1.0 and 2.3 arcmin for precession periods between 235 kyr (secular value) and 328 kyr (instantaneous value) and orbit inclinations ι between 5.3° and 8.6° (Table 2). This large range of values emphasizes the importance of characterizing the Cassini state precisely. For instance, the values obtained from the secular analysis without mutual interactions ($\mu = -2\pi/(235 \text{ kyr})$, $\iota = 5.3^\circ$), $C = 0.34mR^2$ and the Mariner gravity values yield $\theta_{CS} = 1.45$ arcmin using Eq. (12), in good agreement with our numerical solution $\theta_{CS} = 1.49$ arcmin. But this solution is ~ 0.2 arcmin away from the more accurate numerical solution $\theta_{CS} = 1.68$ arcmin. Correct interpretation of future data obtained in support of Peale’s experiment will require the use of the instantaneous Laplace plane and precession rate. With our best fit values for those parameters derived in Section 3.2 (precession period of 328 kyr and inclination $\iota = 8.6^\circ$) and the Mariner 10 C_{20} and C_{22} values, we expect the present obliquity of Mercury to range between 1.60 and 1.87 arcmin depending on the polar moment of inertia.

8. Conclusions

We have investigated several problems related to the spin-orbit motion of Mercury, to the occupancy of the Cassini state, and to the applicability of Peale’s (1976) experiment to the determination of core properties. We have reproduced and augmented the Hamiltonian formalism developed by D’Hoedt and Lemaître (2004) to account for planetary perturbations on the spin-orbit evolution of Mercury. This is accomplished by the addition of a secular potential that captures the long term effects of perturbations of exterior planets on Mercury’s orbit.

The first application of this formalism is an analytical determination of the Laplace plane. The coordinates of the Laplace pole from the purely secular theory are $\lambda_{\text{sec}} = -8.8^\circ$, $\beta_{\text{sec}} = 87.8^\circ$ with a precession period of 235 kyr. We also define an instantaneous Laplace plane and compute its orientation using ephemerides. This instantaneous Laplace pole is the most useful for data interpretation and for numerical integrations since it takes into account the mutual perturbations between planets and does not suffer from the approximations of the secular theory. Our best fit values for the instantaneous Laplace plane are $\lambda_{\text{inst}} = 66.6^\circ$, $\beta_{\text{inst}} = 86.7^\circ$, with a precession period of 328 kyr and an inclination $\iota = 8.6^\circ$. The error bars on these quantities are ~ 50 kyr and 1.2° . However, the equilibrium obliquity [e.g., using Peale’s (1981) equation] is not largely affected by these error bars (uncertainty less than 1 arcsec). We note that the equilibrium obliquity depends strongly on the values assumed for the precession rate and inclination between the orbit and the Laplace planes. For instance, equilibrium obliquity values range from 1.0 to 2.3 arcmin for precession periods from 235 to 328 kyr and for inclinations between 5.3° and 8.6° . This illustrates the importance of choosing the proper Laplace plane and precession period for a correct interpretation of Mercury interior properties in terms of observed spin-orbit parameters. We find an equilibrium obliquity for nominal parameters of $\theta_{CS} = 1.68$ arcmin.

We have developed a set of geometrical constraints and a numerical technique for identifying the position of the Cassini state. The main idea is to start from the known, perturbation-free Cassini state and to turn on planetary perturbations smoothly by gradually increasing the masses of the perturbers. At the end of the integration, one can identify the position of the Cassini state which can be used as a starting point for other integrations.

The Hamiltonian formalism with a particular set of initial conditions can reproduce the numerical results of Rambaux and Bois (2004) that show thousand-year oscillations in the obliquity of Mercury with an amplitude of 1.6 arcmin. We have demonstrated that such oscillations result from the choice of initial conditions rather than from the effect of planetary perturbations. Initial conditions that do not correspond to a Cassini state lead to the introduction of obliquity variations in the form of a free precession, i.e. if Mercury is displaced slightly from the Cassini state, the planet oscillates around it and some free motions appear. The amplitude of the obliquity oscillations is equal to the initial deviation from the Cassini state. If initial conditions representative of a Cassini state are chosen, the spin axis remains very close to the Cassini state, and the obliquity shows no large-amplitude variations.

Our results are obtained without the need for damping or dissipation in the model. The damping period of the free precession is short compared to the age of the Solar System (Peale, 2005), but long compared to the free precession period (~ 1 kyr) and to that of the reorientation of the Laplace plane (~ 10 kyr). The damping has likely lead the spin axis to a spin position very close to that of an instantaneous Cassini state. Once the planet has reached the Cassini state, the torques resulting from tidal dissipation and/or dissipation at a liquid core–solid mantle

boundary will restore the spin to the Cassini state if it is displaced for any reason (Peale, 2005). In the absence of active or recent excitation processes, Mercury's obliquity will therefore remain quasi constant over thousand-year timescales. This configuration satisfies one of the important requirements for the measurement of the size of the core of Mercury with the scheme proposed by Peale (1976).

Acknowledgments

We thank S.J. Peale, P. Nicholson, N. Rambaux, and E.M. Standish for useful discussions, and we also thank E.M. Standish and N. Rambaux for providing numerical values.

References

- Anderson, J.D., Colombo, G., Esposito, P.B., Lau, E.L., Trager, G.B., 1987. The mass, gravity field, and ephemeris of Mercury. *Icarus* 71, 337–349.
- Brouwer, D., Clemence, G.M., 1961. *Methods of Celestial Mechanics*. Academic Press, New York.
- Brouwer, D., van Woerkom, A.J.J., 1950. The secular variations of the orbital elements of the principal planets. *Astron. Pap. Am. Ephem.* 13, 81–107.
- Burns, J.A., Hamill, P., Cuzzi, J.N., Durisen, R.H., 1979. On the 'thickness' of Saturn's rings caused by satellite and solar perturbations and by planetary precession. *Astron. J.* 84, 1783–1801.
- Colombo, G., 1966. Cassini's second and third laws. *Astron. J.* 71, 891–896.
- Deprit, A., 1967. Free rotation of a rigid body studied in the phase plane. *Am. J. Phys.* 35, 424–428.
- D'Hoedt, S., Lemaître, A., 2004. The spin-orbit resonant rotation of Mercury: A two degree of freedom Hamiltonian model. *Celest. Mech. Dynam. Astron.* 89, 267–283.
- Gladman, B., Quinn, D.D., Nicholson, P., Rand, R., 1996. Synchronous locking of tidally evolving satellites. *Icarus* 122, 166–192.
- Harder, H., Schubert, G., 2001. Sulfur in Mercury's core? *Icarus* 151, 118–122.
- Laskar, J., 1988. Secular evolution of the Solar System over 10 million years. *Astron. Astrophys.* 198, 341–362.
- Milani, A., Rossi, A., Vokrouhlický, D., Villani, D., Bonanno, C., 2001. Gravity field rotation state of Mercury from the BepiColombo radio science experiments. *Planet. Space Sci.* 49, 1579–1596.
- Murray, C.D., Dermott, S.F., 1999. *Solar System Dynamics*. Cambridge Univ. Press, Cambridge, UK.
- Owen, W.M., 1990. A theory of the Earth's precession relative to the invariable plane of the Solar System. Ph.D. thesis. Florida University, Gainesville.
- Peale, S.J., 1969. Generalized Cassini's laws. *Astron. J.* 74, 483–489.
- Peale, S.J., 1974. Possible histories of the obliquity of Mercury. *Astron. J.* 79, 722–744.
- Peale, S.J., 1976. Does Mercury have a molten core. *Nature* 262, 765–766.
- Peale, S.J., 1981. Measurement accuracies required for the determination of a mercurian liquid core? *Icarus* 48, 143–145.
- Peale, S.J., 1988. The rotational dynamics of Mercury and the state of its core. In: Vilas, F., Chapman, C.R., Matthews, M.S. (Eds.), *Mercury*. Univ. of Arizona Press, Tucson, AZ, pp. 461–493.
- Peale, S.J., 2005. The free precession and libration of Mercury. *Icarus* 178, 4–18.
- Peale, S.J., 2006. The proximity of Mercury's spin to Cassini State 1 from adiabatic invariance. *Icarus* 181, 338–347 (this issue).
- Peale, S.J., Phillips, R.J., Solomon, S.C., Smith, D.E., Zuber, M.T., 2002. A procedure for determining the nature of Mercury's core. *Meteorit. Planet. Sci.* 37, 1269–1283.
- Pettengill, G.H., Dyce, R.B., 1965. A radar determination of the rotation of the Planet Mercury. *Nature* 206, 1240.
- Rambaux, N., Bois, E., 2004. Theory of the Mercury's spin-orbit motion and analysis of its main librations. *Astron. Astrophys.* 413, 381–393.
- Standish, E.M., Newhall, X.X., Williams, J.G., Yeomans, D.K., 1992. Orbital ephemerides of the Sun, Moon and planets. In: Seidelmann, P.K. (Ed.), *Explanatory Supplement to the Astronomical Almanac*. University Science Books, Mill Valley, CA, pp. 279–323.
- Solomon, S.C., and 20 colleagues, 2001. The MESSENGER mission to Mercury: Scientific objectives and implementation. *Planet. Space Sci.* 49, 1445–1465.
- Ward, W.R., 1975. Tidal friction and generalized Cassini's laws in the Solar System. *Astron. Astrophys.* 80, 64–70.